

## SECOND ORDER ANALYSIS FOR A COMPACT PROTON SYNCHROTRON

Hisaharu Sakae, Yasuyuki Miyauchi, Mitsuru Ogoshi, Shin-ichi Mandai  
Advanced Technology Development Department  
Ishikawajima-Harima Heavy Industries Co., Ltd  
1-6-2, Marunouchi, Chiyoda-ku, Tokyo 100, Japan  
Makoto Inoue, Akira Noda  
Accelerator Laboratory, Institute for Chemical Research  
Kyoto University  
Gokanoshō, Uji-shi, Kyoto 611, Japan

### ABSTRACT

A second order particle tracking for a prototype compact proton synchrotron dedicated to medical use has been performed. The calculations have been done for a square FDDF lattice and a conventional FODO lattice for comparison. In this analysis it is found that the second order effect causes the beam position shift and the spread of beam size in the early stage of circulation and the second order effect to the FDDF lattice is lower than that to the FODO lattice.

### INTRODUCTION

It is generally known that an intermediate energy proton beam (70~250 [MeV]) is effective for cancer control, and a compact proton synchrotron dedicated to proton therapy has been designed [1]. In that design, a square FDDF lattice (Chasman-Green like lattice) and a square FODO lattice were compared from the view point of reducing the size of circulating proton beam and the former one (FDDF) is considered to be preferable as the candidate.

Though, the preliminary design has been performed by calculations with the linear optics code, it is also necessary to check the higher order effects due to the small bending radius. Hence, the second order analysis has been done in order to estimate the second order effect and ascertain the validity of above mentioned lattice selection.

### LATTICE DESCRIPTION AND MACHINE PARAMETERS

The lattice design is given below and its detailed description is given in ref.[1].

A schematic lattice layout of a square FDDF lattice is shown in Fig.1, and its lattice specifications and machine parameters are listed in Table 1 and 2. The lattice is a square with four 90 [deg] sector bending magnets. The radius of curvature and magnetic field of bending magnets (BM) are 1.8 [m] and 1.35 [T], respectively. Doublets of quadrupole magnets (QF : focusing, QD : defocusing) are located at both ends of each straight section. Changing the field gradients of these magnets, following two operating modes can be selected: (1) a FDDF symmetrical mode with superperiodicity of 4 (abbreviated as S-mode), and (2) a Chasman-Green mode with superperiodicity of 2 (abbreviated as CG-mode). For the medical use proton synchrotron, the extraction beam energy of about 250 [MeV] is suitable for full depth proton therapy, and averaged proton beam current of more than 10 [nA] is required.

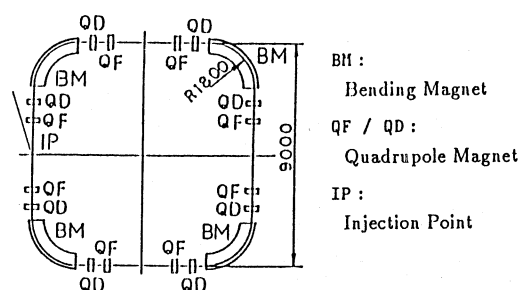


Fig.1 : FDDF lattice layout

Table 1 : Proton Synchrotron Lattice Specifications

Injection energy	7 [MeV]	(114.8 [MeV/c])
Extraction energy	250 [MeV]	(729.1 [MeV/c])
Superperiodicity	S-mode : 4	CG-mode : 2
Betatron tunes (H/V)	2.20 / 1.15	
Bending field	1.35 [T]	
Quadrupole field (F/D)	S-mode	8.25 / -7.30 [T/m]
	CG-mode	9.52 / -8.19 [T/m]
		7.10 / -6.32 [T/m]

Table 2 : Machine Parameters

		S-mode	CG-mode	FODO
$\nu_x / \nu_y$		2.20/1.15	2.20/1.15	1.85/1.20
$\beta_x$	[m]	1.70~3.34	1.46~3.13	1.57~3.50
	IP [m]	2.04	1.90	2.01
$\beta_y$	[m]	2.42~8.72	1.89~9.20	2.19~10.4
	IP [m]	2.42	1.89	2.50
$\alpha_x$	[m]	0.00	0.00	-1.05~1.72
	IP [m]	0.00	0.00	-0.54
$\alpha_y$	[m]	0.00	0.00	-6.64~1.94
	IP [m]	0.00	0.00	-0.38
$\eta_x$	[m]	0.15~1.87	0.00~3.92	0.82~2.19
	IP [m]	1.87	0.00	1.87

## SECOND ORDER PARTICLE TRACKING

A particle tracking is performed by solving the equation of motion directly [2]. Transfer of a particle can be expanded as follows:

$$x_i(s) = \sum_{j=1}^6 R_{ij} x_j(0) + \sum_{j=1}^6 \sum_{k=1}^6 T_{ijk} x_j(0) x_k(0) + \dots \quad (1)$$

where variables  $x_i$  ( $i = 1 \sim 6$ ) denote the coordinates  $x$ ,  $x'$  (horizontal position and momentum),  $y$ ,  $y'$  (vertical position and momentum),  $\ell$  (bunch length) and  $\delta = \Delta p/p_0$  (momentum dispersion). The term  $R_{ij}$  and  $T_{ijk}$  are the first and the second order coefficients of expansion, respectively. The second order effect of bending radius comes out of the terms  $T_{ijk}$ .

The tracking has been performed by using Eq.(1) for following three cases: (1) a square FDDF lattice with S-mode, (2) a square FDDF lattice with CG-mode and (3) FODO lattice for comparison (see ref.[1]). In order to estimate the second order effects on the preliminary design and calculation, this calculation has taken no sextupole components of the field of all magnets into account. The transfer matrices  $R_{ij}$  and  $T_{ijk}$  for each case have been calculated by using the second order lattice design code DIMAD [3]. The starting point of tracking (i.e. injection point) is set at the center of the straight section. For the lattice of S-mode and CG-mode, Twiss parameters  $\alpha_x$  and  $\alpha_y$  are set to be zero at this point. In the CG-mode, dispersion function  $\eta_x$  is also zero. The starting coordinates of tracking particles are distributed in the ellipses of the phase space given by Twiss parameters and emittance at random. Horizontal and vertical emittance are set to  $123\pi$  and  $12.3\pi$  [mm-mrad], respectively. The maximum value of these coordinates are listed in Table 3. The number of calculated particles is 1,000 and the momentum dispersion is set to be 0.3 %.

Table 3 : Injection Beam Coordinates

	S-mode	CG-mode	FODO
$x_{\max}$ [mm]	15.8	15.3	15.7
$x'_{\max}$ [mrad]	5.44	4.81	5.54
$y_{\max}$ [mm]	7.76	8.04	8.88
$y'_{\max}$ [mrad]	2.25	2.55	2.37

## RESULTS OF PARTICLE TRACKING

Total number of circulating particles in the acceptance during 5,000 turns are shown in Fig.2. For both modes of the FDDF lattice, total numbers of circulating beams seem to saturate after rapid decay of initial 1,000~2,000 revolutions and 80 % of initial particles survive at 5,000 turns. On the contrary, only 50 % of initial particles can survive for the FODO lattice and further decreasing of particles number is expected after 5,000 turns.

Figure 3 shows that the variation of horizontal beam center. Horizontal beam center of CG-mode oscillates in the range of  $\pm 2.0$  [mm] and this value is the smallest among three cases. For S-mode and FODO lattice, horizontal beam center is biased to positive side (the direction of the lattice center).

The variation of horizontal beam size is shown in Fig.4. Horizontal beam broadening in 200 turns can be found in S-mode and CG-mode and

it becomes almost constant ( $\sim 4.0$  [cm]) after 200 turns. In the FODO lattice, beam shrinks after reaching maximum value ( $\sim 5.5$  [cm]). It was explained by the considerable reduction of surviving particles number.

As shown in Figs. 5 and 6, the variation of vertical beam center and beam size of CG-mode are also the smallest among these of three cases.

## SUMMARY AND DISCUSSION

In this analysis, it was found that in the early stage of circulation the second order effect causes the beam position shift and the beam spread that can not be found in the linear analysis. The second order effect to a square FDDF lattice (specially in CG-mode) is less than that to a FODO lattice. It may be perceived that relatively large mean dispersion of a FODO lattice causes larger second order effects than for a FDDF lattice.

For detailed design of accelerator components and the selection of the operating modes of the synchrotron, further analysis of the effect of higher order multipole components of magnetic field is necessary.

## ACKNOWLEDGMENT

The authors would like to express their sincere thanks to Dr. F. Jones for courteously providing the code DIMAD.

## REFERENCES

- [1] Y. Miyauchi et al., "Design Study of Proton Synchrotrons for Medical Use at Kyoto University", in this proceedings (1991).
- [2] K. L. Brown et al., "First- and Second-Order Charged Particle Optics", AIP-127 (1985).
- [3] R. V. Servranckx et al., "Users Guide to the Program DIMAD", SLAC-285 UC-28 (1985).

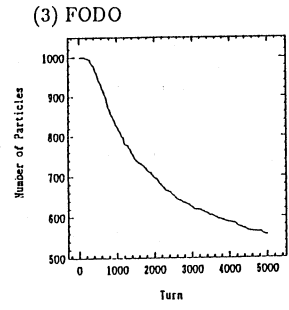
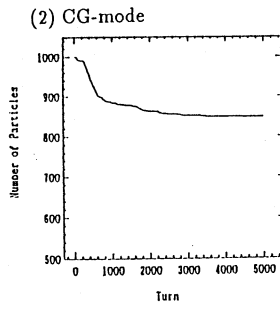
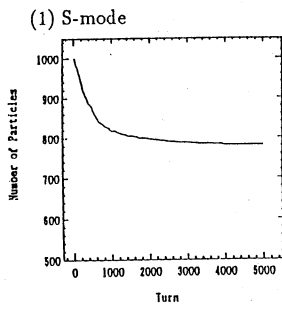


Fig.2 : Total Number of Particles

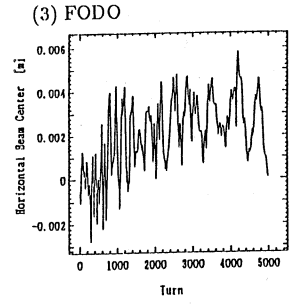
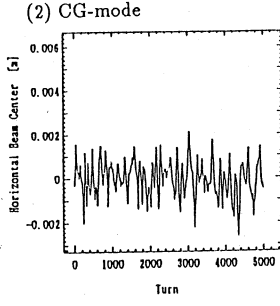
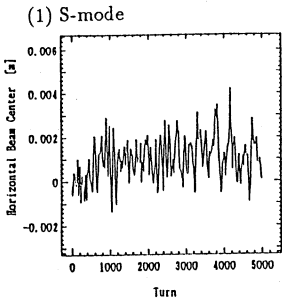


Fig.3 : Horizontal Beam Center

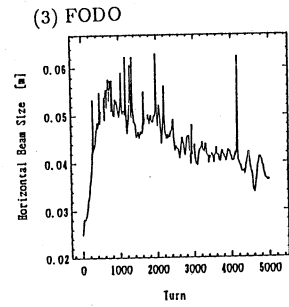
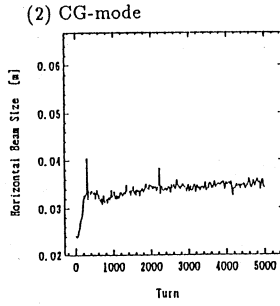
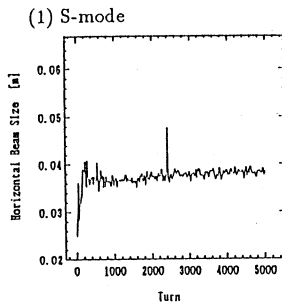


Fig.4 : Horizontal Beam Size

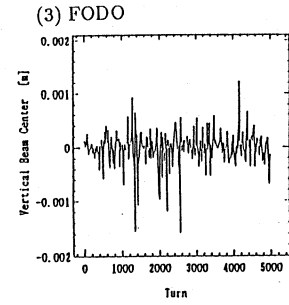
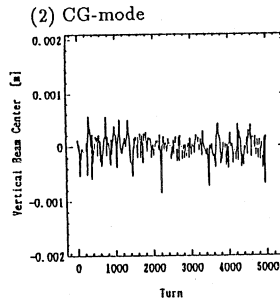
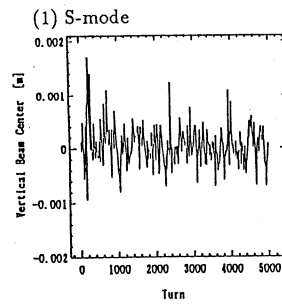


Fig.5 : Vertical Beam Center

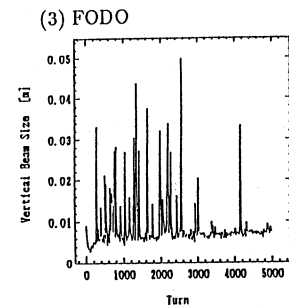
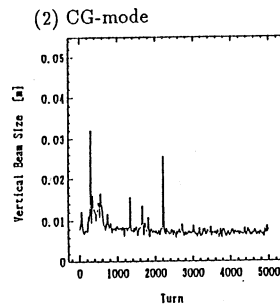
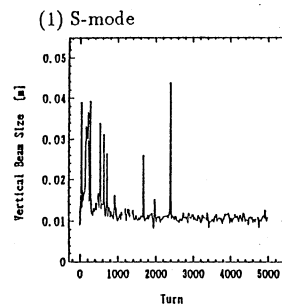


Fig.6 : Vertical Beam Size